Inorganic Chemistry
Article

Inorg. Chem. **2009**, *48*, 6297–6302 **6297**
DOI: 10.1021/ic900633k

Formation and Calculations of the Simple Terminal Triplet Pnictinidene Molecules $N{\div}MF_3$, $P{\div}MF_3$, and $As{\div}MF_3$ (M = Ti, Zr, Hf)

Xuefeng Wang, Jonathan T. Lyon, and Lester Andrews*

Department of Chemistry, University of Virginia, P.O. Box 400319, Charlottesville, Virginia 22904-4319

Received March 31, 2009

Laser-ablated Ti, Zr, and Hf atoms react with NF_3, PF_3, or AsF_3 to produce triplet state terminal pnictinidene $N{\div}MF_3$, $P{\div}MF_3$, or $As{\div}MF_3$ molecules, which are trapped in an argon matrix. Products are identified from infrared spectra and comparison to theoretically predicted vibrations. Density functional theory calculations converge to C_{3v} symmetry structures for these lowest energy products. The two unpaired electrons in nitrogen 2p, phosphorus 3p, or arsenic 4p orbitals are shared in different small amounts with empty metal *n*d orbitals leading to very weak degenerate $\pi\alpha$ molecular orbitals based on bonding orbital analysis and spin density calculations. This weak π bonding interaction with early transition metal group 4 *n*d orbitals is optimum for Zr with phosphorus 3p orbitals.

Introduction

Nitrenes, compounds of the general formula R-N, are analogues of carbenes, and both generally function as reactive intermediates. The common source of nitrenes is the photolysis of azides.[1] Most nitrenes have triplet ground states, and $CH_3{-}N$ is a simple example.[2,3] A characteristic reaction of alkyl nitrenes is substituent rearrangement to give the imine.[1] Methylene imine $CH_2{=}NH$ is a well-known more stable isomer of triplet $CH_3{-}N$.[4,5] The more stable perfluoro analogue $CF_2{=}NF$ is easier to investigate by experiment,[6,7] and the $CF_3{-}N$ isomer has recently been observed in the triplet ground-state by matrix isolation electron spin resonance methods.[8] These two isomers have approximately the same energy within the error of calculations. We have been unable to find experimental evidence for phosphorus or arsenic analogues of the simple above reactive intermediates. Such terminal pnictinidenes tend to coordinate with formal double bonding to organometallic fragments,[9] but under matrix isolation conditions the terminal pnictinidene can be isolated and characterized. Examples of related molecules include the phospha- and arsaalkenes $CF_3P{=}CF_2$ and $CF_3As{=}CF_2$, $RE{=}C(NMe_2)_2$, (E = P, As) and phosphinidene complexes.[10,11]

Reactions of laser ablated group 4 transition metal atoms with ammonia have prepared transition metal imine analogues $MH_2{=}NH$, which were characterized by matrix infrared spectra and density functional calculations.[12,13] The analogous reactions of ammonia with Mo and W metal atoms produced instead the lower energy $MH_3{\equiv}N$ terminal metal nitrides. However, the greater stability of metal fluoride bonds supported the formation of the Cr, Mo, and W trifluoro derivatives $MF_3{\equiv}N$ and the phosphide species for Mo and W in the analogous reactions with NF_3 and PF_3.[14,15] Reactions with arsenic trifluoride followed suit with terminal arsenides for Mo and W.[16] Accordingly, group 4 metal atom reactions with NF_3, PF_3, and AsF_3 were performed to seek the novel trifluorometal triplet state pnictinidenes $MF_3{-}N$, $MF_3{-}P$, and $MF_3{-}As$, and a combined experimental and theoretical investigation is reported here. Hereafter, we will use the $E{\div}MF_3$ notation to indicate these triplet ground-state product group 15 non-metal and group 4 transition metal containing molecules.

* To whom correspondence should be addressed. E-mail: lsa@virginia.edu.

(1) Carey, F. A.; Sundberg, R. J. *Advanced Organic Chemistry, Part B: Reactions and Synthesis*, 4th ed.; Kluwer Academic/Plenum Publishers: New York, 2001.
(2) Chappell, E. L.; Engelking, P. C. *J. Chem. Phys.* **1988**, *89*, 6007.
(3) Ferrante, R. F. *J. Chem. Phys.* **1991**, *94*, 4678.
(4) Pearson, R.; Lovas, F. *J. Chem. Phys.* **1977**, *66*, 4149.
(5) De Oliveira, O.; Martin, J. M. L.; Silwel, I. K. C.; Liebman, J. F. *J. Comput. Chem.* **2001**, *22*, 1297.
(6) Christen, D.; Oberhammer, H.; Hammaker, R. M.; Chang, S. C.; Desmarteau, D. D. *J. Am. Chem. Soc.* **1982**, *104*, 6186.
(7) Bock, H.; Dammel, R.; Desmarteau, D. D. *Z. Naturforsch.* **1987**, *42b*, 308.
(8) Gritsan, N. P.; Likhotvorik, I.; Zhu, Z.; Platz, M. S. *J. Phys. Chem. A* **2001**, *105*, 3039.
(9) Cowley, A. H. *Acc. Chem. Res.* **1997**, *30*, 445.
(10) (a) Steger, B.; Oberhammer, H.; Grobe, J.; Levan, D. *Inorg. Chem.* **1986**, *25*, 3177. (b) Weber, L. *Eur. J. Inorg. Chem.* **2007**, 4095.
(11) Cossairt, B. M.; Cummins, C. C. *Inorg. Chem.* **2008**, *47*, 9363.
(12) Chen, M.; Lu, H.; Dong, J.; Miao, L.; Zhou, M. *J. Phys. Chem. A* **2002**, *106*, 11456.
(13) Zhou, M.; Chen, M.; Zhang, L.; Lu, H. *J. Phys .Chem. A* **2002**, *106*, 9017.
(14) Wang, X.; Andrews, L. *Organometallics* **2008**, *27*, 4885.
(15) Wang, X.; Andrews, L.; Lindh, R.; Veryazov, V.; Roos, B. O. *J. Phys. Chem. A* **2008**, *112*, 8030.
(16) Wang, X.; Andrews, L.; Knitter, M.; Malmqvist, P.-Å.; Roos, B. O. *J. Phys. Chem. A* **2009**, *113*, DOI: 10.1021/jp901308n, in press.

Published on Web 04/29/2009

Experimental and Computational Methods

Laser ablated Ti (Goodfellow), Zr, and Hf (Johnson-Matthey) atoms were reacted with NF_3 (Matheson), PF_3 (PCR Research), or AsF_3 (Ozark-Mahoning, vacuum distilled from dry NaF) in excess argon during condensation at 5−8 K using closed-cycle refrigerators described elsewhere.[17,18] Reagent gas mixtures were typically 0.5% in argon and the laser ablated metal atom concentrations were much lower. After reaction, infrared spectra were recorded at a resolution of 0.5 cm^{-1} using Nicolet 550 or 750 spectrometers with Hg−Cd−Te B range detectors. Samples were later irradiated for 15 min periods by a mercury arc street lamp (175 W) with the globe removed using a combination of optical filters, and then samples were annealed to allow reagent diffusion and further reaction.

Following our work on reactions with the isoelectronic fluoroform molecule, theoretical computations were performed using the Gaussian 03 program with the B3LYP hybrid density functional and some comparisons with the BPW91 functional.[19−21] The 6-311 + G(2d) basis was used to represent the electronic density of nitrogen, fluorine, phosphorus, and arsenic atoms, and SDD pseudopotentials were used for the metal atoms.[22,23] Frequencies were computed analytically, and all energy values reported include zero-point vibrational corrections. The calculation of vibrational frequencies is not an exact science, and density functional theory (DFT) provides a very good approximation for observed frequencies. Calculated frequencies are usually a few percent higher than observed values,[24,25] but that is not always the case. Finally, bonding analysis was done using the natural bond orbital method in Gaussian 03.[19,26]

Results and Discussion

Infrared spectra of products formed in the reactions of laser-ablated titanium, zirconium, and hafnium atoms with NF_3, PF_3, and AsF_3 in excess argon during condensation at 5−8 K will be presented in turn. Density functional calculations were performed to support the identifications of new reaction products. Bands common to experiments using different laser ablated metals with NF_3 [such as NF_2 and NF_2^-], with PF_3 [PF_2, PF_5, and PF_2^-], and with AsF_3 [AsF_2 and AsF_5] have been identified previously and will not be mentioned again here.[15,27,28]

Infrared Spectra. Sets of infrared spectra for Ti, Zr, and Hf reactions with NF_3 are compared in Figure 1. The strong bands at 791.8 and 740.2 cm^{-1} in the Ti reaction, trace (a), have been reported previously and assigned to

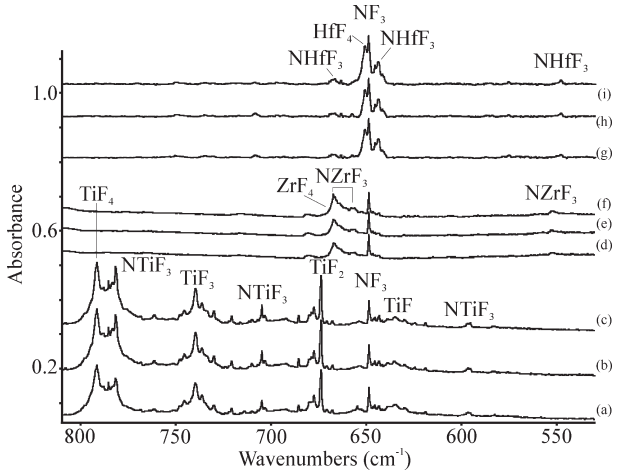

Figure 1. Infrared spectra for group 4 metal atom reaction products with NF_3 in excess argon in the 810−530 cm^{-1} region. (a) Spectrum after co-deposition of laser-ablated Ti and NF_3 at 0.5% in argon at 8 K for 60 min, (b) after >220 nm irradiation for 20 min, (c) after annealing to 30 K, and (d) spectrum after co-deposition of laser-ablated Zr and NF_3 at 0.5% in argon at 8 K for 60 min, (e) after >290 nm irradiation, and (f) after >220 nm irradiation, and (g) spectrum after co-deposition of laser-ablated Hf and NF_3 at 0.5% in argon at 8 K for 60 min, (h) after annealing to 20 K, and (i) after >220 nm irradiation.

binary titanium fluoride species as have the weaker bands at 677.7, 674.0, and 643.6 cm^{-1}.[29,30] The latter assignments were made to these products from the thermal Ti atom reaction with argon/fluorine samples. New bands at 782.1, 705.1, and 596.7 cm^{-1} increase 30% on full arc (>220 nm) irradiation, and sharpen on annealing to 30 K, spectra (b) and (c). The major Zr reaction product at 667.4 cm^{-1} is joined by weaker 658.2 and 553.1 cm^{-1} bands, which increase in concert 10% on >290 nm irradiation and another 30% on >220 nm irradiation, scans (d,e,f). The shoulder absorption at 668.6 cm^{-1} is in agreement with the major product from an experiment with Zr and F_2 in excess argon performed in this laboratory and is near the 668.0 cm^{-1} band observed earlier for ZrF_4.[31] The strongest Hf product band shifts lower to 650.8 cm^{-1} just above the NF_3 absorption at 648.9 cm^{-1}, but this is in precise agreement with our major band for the Hf and F_2 reaction and appropriate for HfF_4.[31] Comparison with the zirconium experiment suggests that there is a major product absorption at 643.9 cm^{-1} with weaker associated 666.7 and 548.1 cm^{-1} bands that increase together 20% on >20 K annealing and another 20% on >220 nm irradiation, spectra (g,h,i).

Infrared spectra for the corresponding group 4 metal atom reactions with PF_3 are illustrated in Figure 2. The TiF_3 and TiF_2 bands were barely detected as PF_3 is a more stable compound than NF_3. The major Ti reaction product at 769.0 cm^{-1} is joined by a weaker band at 688.2 cm^{-1}, and these two bands increase 30% on >290 nm irradiation and reduce a like amount on subsequent >220 nm irradiation, traces (a,b,c). With Zr the strong product

(17) (a) Andrews, L. *Chem. Soc. Rev.* **2004**, *33*, 123. (b) Andrews, L.; Citra, A. *Chem. Rev.* **2002**, *102*, 885.
(18) Andrews, L.; Cho, H.-G. *Organometallics* 2006, *25*, 4040, and references therein (Review article).
(19) Frisch, M. J., et al. *Gaussian 03*, Revision D.01; Gaussian, Inc.: Pittsburgh, PA, 2004.
(20) (a) Becke, A. D. *J. Chem. Phys.* **1993**, *98*, 5648. (b) Lee, C.; Yang, Y.; Parr, R. G. *Phys. Rev. B* **1988**, *37*, 785.
(21) Perdew, J. P.; Burke, K.; Wang, Y. *Phys. Rev. B* 1996, *54*, 16533, and references therein.
(22) Frisch, M. J.; Pople, J. A.; Binkley, J. S. *J. Chem. Phys.* **1984**, *80*, 3265.
(23) Andrae, D.; Haeussermann, U.; Dolg, M.; Stoll, H.; Preuss, H. *Theor. Chim. Acta* **1990**, *77*, 123.
(24) Scott, A. P.; Radom, L. *J. Phys. Chem.* **1996**, *100*, 16502.
(25) Andersson, M. P.; Uvdal, P. L. *J. Phys. Chem. A* **2005**, *109*, 2937.
(26) (a) Reed, A. E.; Weinstock, R. B.; Weinhold, F. *J. Chem. Phys.* **1985**, *83*, 735. (b) Reed, A. E.; Curtiss, L. A.; Weinhold, F. *Chem. Rev.* **1988**, *88*, 899.
(27) Jacox, M. E. *J. Phys. Chem. Ref. Data* 1994, Monograph 3; 1998, *27* (2), 115.
(28) (a) Khider Aljibury, A. J.; Redington, R. L. *J. Chem. Phys.* **1970**, *52*, 453. (b) Brum, J. L.; Hudgens, J. W. *J. Chem. Phys.* **1997**, *106*, 485.
(29) Hastie, J. W.; Hauge, R. H.; Margrave, J. L. *J. Chem. Phys.* **1969**, *51*, 2648.
(30) Wilson, A. V.; Roberts, A. J.; Young, N. A. *Angew. Chem., Int. Ed.* **2008**, *47*, 1774.
(31) (a) Büchler, A.; Berkowitz-Mattuck, J. B.; Dugre, D. H. *J. Chem. Phys.* **1961**, *34*, 2202. (b) Hauge, R. H.; Margrave, J. L. *High Temp. Sci.* **1973**, *5*, 89. (c) unpublished infrared spectra of Zr and Hf reaction products with F_2 in excess argon at 5 K.

Table 1. Observed and Calculated Fundamental Frequencies of the N÷MF_3 Nitrene Complexes in the Ground $^3A_1$ Electronic States with C_{3v} Structures[a]

	N÷TiF_3			N÷ZrF_3			N÷HfF_3			N÷HfF_3 (BPW91)	
approx. mode description	obs	calc	int	obs	calc	int	obs	calc	int	calc	int
M−F str, a_1							666.7	645	34	630	30
M−F str, e	782.1[b]	796	255 × 2	667.4[c]	669	208 × 2	643.9	639	156 × 2	626	142 × 2
M−F str, a_1	705.1[b]	719	102	658.2	647	61					
N÷M str, a_1	596.7	629	29	553.1	565	58	548.1	550	49	537	39
MF_3 def, e		203	15 × 2		168	22 × 2		162	3 × 2	162	4 × 2
MF_3 def, a_1		190	21		152	26		141	23	138	19
N−M−F def, e		176	1 × 2		155	6 × 2		152	24 × 2	150	16 × 2

[a] Frequencies and intensities are in cm^{-1} and km/mol. Observed in an argon matrix. Frequencies and intensities computed with B3LYP/6-311+G(2d) in the harmonic approximation using the SDD core potential and basis set for metal atoms. Calculations using the BPW91 functional gave similar frequencies as shown for the hafnium product. [b] The mode symmetry notations are based on the C_{3v} structure. [c] Band probably over some ZrF_4 absorption.

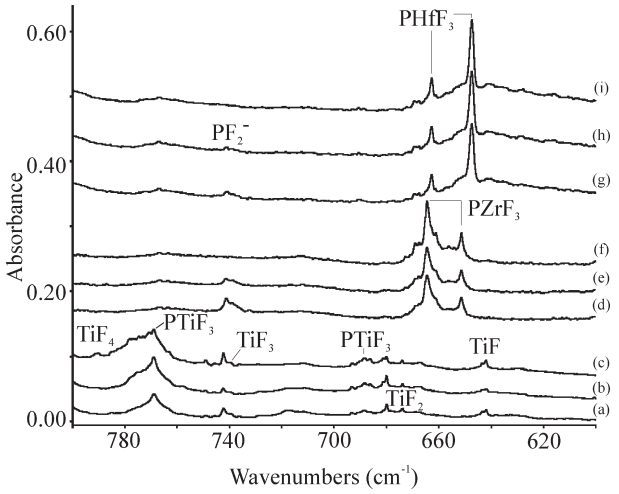

Figure 2. Infrared spectra for group 4 metal atom reaction products with PF_3 in excess argon in the 800−600 cm^{-1} region. (a) Spectrum after co-deposition of laser-ablated Ti and PF_3 at 0.5% in argon at 8 K for 60 min, (b) after 290 nm irradiation for 20 min, and (c) after >220 nm irradiation for 20 min. (d) Spectrum after co-deposition of laser-ablated Zr and PF_3 at 0.13% in argon at 8 K for 60 min, (e) after >290 nm irradiation, and (f) after >220 nm irradiation. (g) Spectrum after co-deposition of laser-ablated Hf and PF_3 at 0.5% in argon at 8 K for 60 min, (h) after >290 nm irradiation, and (i) after >220 nm irradiation.

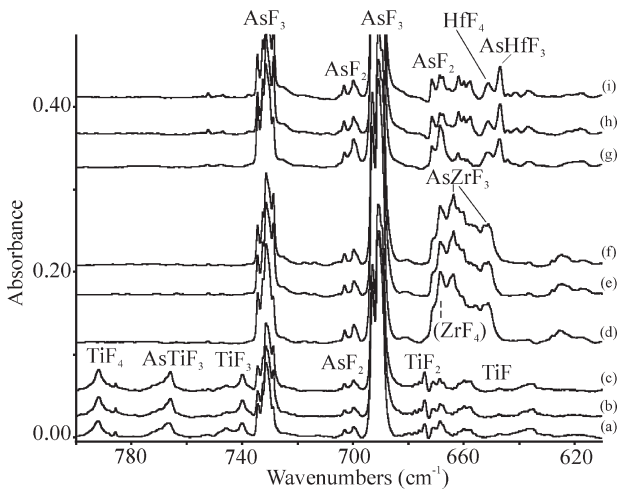

Figure 3. Infrared spectra for group 4 metal atom reaction products with AsF_3 in excess argon in the 800−610 cm^{-1} region. (a) Spectrum after co-deposition of laser-ablated Ti and AsF_3 at 0.5% in argon at 5 K for 60 min, (b) after 290 nm irradiation for 20 min, and (c) after >220 nm irradiation for 20 min. (d) Spectrum after co-deposition of laser-ablated Zr and AsF_3 at 0.13% in argon at 5 K for 60 min, (e) after >290 nm irradiation, and (f) after >220 nm irradiation. (g) Spectrum after co-deposition of laser-ablated Hf and AsF_3 at 0.5% in argon at 5 K for 60 min, (h) after >290 nm irradiation, and (i) after >220 nm irradiation.

bands at 664.2 and 651.4 cm^{-1} were very intense (absorbance 0.2 and 0.1, respectively) using 0.5% precursor in argon, so the sample was diluted to 0.13%, and these bands with the same relative intensity are shown in Figure 2. The 664.2 and 651.4 cm^{-1} bands were not changed on the initial >290 nm irradiation but increased together 50% on the next >220 nm irradiation, spectra (d,e,f). Using Hf the product band relative intensities reverse at 662.6 and 647.4 cm^{-1}, and these bands increase 10% on >290 nm irradiation and another 20% on >220 nm irradiation, scans (g,h,i).

Spectra for group 4 metal reactions with AsF_3 are shown in Figure 3. The bands at 791.8, 740.2, and 674.2 cm^{-1} in the Ti reaction for $TiF_{4,3,2}$ are weaker than with NF_3, and a new absorption was observed at 765.9 cm^{-1}. The corresponding band for Zr is 663.6 cm^{-1}, and ZrF_4 absorption underneath increases the AsF_2 peak at 668.6 cm^{-1}. Using Hf the HfF_4 band is observed at 651.0 cm^{-1} and the new product lower at 646.9 cm^{-1}.

Identification of the N÷MF_3 molecules. Reactions of Ti, Zr, and Hf atoms with NF_3 gave new strong, medium, and weak product absorptions with each metal, which are compared in Table 1 with frequencies calculated for the lowest energy product molecule. The metal atom reaction with NF_3 most likely proceeds through an insertion step like the halomethane reactions investigated extensively in this laboratory,[32] and here the reaction proceeds from the difluoroamine inserted species to the fluoroimine and then to the nitrene species. These steps in the reaction are 216, 235, and 274 kcal/mol lower in energy than the initial reactants Ti and NF_3, respectively. The zirconium fluoroimine and nitrene species are 266 and 313 kcal/mol lower energy than the combined reagents, and the analogous hafnium products are 261 and 319 kcal/mol lower than the starting materials.

$$M(^3F) + NF_3 \rightarrow F_2N-MF \rightarrow FN{=}MF_2 \rightarrow N \div MF_3 \quad (1)$$

Our experience with Ti−F, Zr−F, and Hf−F stretching frequencies is that the B3LYP calculated values slightly exceed the argon matrix observed values by about 5% for

(32) Lyon, J. T.; Andrews, L. *Inorg. Chem.* 2007, *46*, 568. (Gr. 4 + fluoromethanes).

Table 2. Observed and Calculated Fundamental Frequencies of the P÷MF_3 Complexes in the Ground $^3A_1$ Electronic States with C_{3v} Structures[a]

	P÷TiF_3			P÷ZrF_3			P÷HfF_3			P÷HfF_3 (BPW91)	
approx. mode description	obs	calc	int	obs	calc	int	obs	calc	int	calc	int
M−F str, a_1							662.6	639	10	625	67
M−F str, e	769.0	785	219 × 2	664.2	665	181 × 2	647.4	635	138 × 2	623	124 × 2
M−F str, a_1	688.2	699	138	651.4	640	98					
P÷M str, a_1		369	28		330	32		308	20	304	17
MF_3 def, e		193	8 × 2		167	11 × 2		158	9 × 2	155	7 × 2
MF_3 def, a_1		172	11		146	15		138	16	132	13
P−M−F def, e		133	0 × 2		115	3 × 2		111	3 × 2	107	4 × 2

[a] Frequencies and intensities are in cm^{-1} and km/mol. Observed in an argon matrix. Frequencies and intensities computed with B3LYP/6-311+G(2d) in the harmonic approximation using the SDD core potential and basis set for metal atoms. Calculations using the BPW91 functional gave similar frequencies as shown for the hafnium product. The mode symmetry notations are based on the C_{3v} structure.

Table 3. Observed and Calculated Fundamental Frequencies of the As÷MF_3 Complexes in the Ground $^3A_1$ Electronic States with C_{3v} Structures[a]

	As÷TiF_3			As÷ZrF_3			As÷HfF_3			As÷HfF_3 (BPW91)	
approx. mode description	obs	calc	int	obs	calc	int	obs	calc	int	calc	int
M−F str, a_1							n o.	639	78	625	74
M−F str, e	765.9	783	209 × 2	663.6	664	173 × 2	646.9	635	133 × 2	622	120 × 2
M−F str, a_1	n.o.	697	147	651.1	640	108					
As÷M str, a_1		295	24		246	26		214	16	210	13
MF_3 def, e		192	7 × 2		167	11 × 2		162	10 × 2	155	7 × 2
MF_3 def, a_1		148	6		132	9		133	10	125	8
As−M−F def, e		117	0 × 2		100	2 × 2		100	2 × 2	92	2 × 2

[a] Frequencies and intensities are in cm^{-1} and km/mol. Observed in an argon matrix. Frequencies and intensities computed with B3LYP/6-311+G(2d) in the harmonic approximation using the SDD core potential and basis set for metal atoms. Calculations using the BPW91 functional gave similar frequencies as shown for the hafnium product. The mode symmetry notations are based on the C_{3v} structure.

Table 4. Structural Parameters and Physical Constants for Triplet State Pnictinidenes E÷MF_3 (E = N, P, As, M = Ti, Zr, Hf) in C_{3v} Symmetry[a]

parameter	N÷TiF_3	P÷TiF_3	As÷TiF_3	N÷ZrF_3	P÷ZrF_3	As÷ZrF_3	N÷HfF_3	P÷HfF_3	As÷HfF_3
r(E÷M)	1.959	2.426	2.530	2.143	2.606	2.715	2.146	2.609	2.715
r(M−F)	1.756	1.759	1.759	1.925	1.926	1.925	1.922	1.923	1.922
<(EMF)	105.8	105.4	105.2	106.8	106.8	107.0	106.5	106.8	107.0
q(E)[b]	−0.19/−0.19	0.06/0.14	0.003/0.16	−0.44/−0.42	−0.22/−0.08	−0.27/−0.05	−0.42/−0.45	−0.08/−0.13	−0.18/−0.09
q(M)[b]	1.14/1.60	0.80/1.27	0.82/1.25	1.62/2.27	1.39/192	1.43/1.99	1.50/2.38	1.10/2.04	1.16/2.01
q(F)[b]	−0.32/−0.47	−0.28/−0.47	−0.27/−0.47	−0.39/−0.62	−0.39/−0.61	−0.39/−0.61	−0.36/−0.64	−0.34/−0.64	−0.33/−0.64
E(s)[c]	1.89	1.90	1.92	1.91	1.91	1.93	1.91	1.91	1.92
E(p)[c]	3.30	2.95	2.91	3.49	3.15	3.11	3.53	3.20	3.15
M(s)[c]	0.16	0.28	0.29	0.15	0.27	0.28	0.21	0.33	0.35
M(d)[c]	1.97	2.10	2.10	1.38	1.55	1.55	1.22	1.35	1.35
M(p)[c]	0.73	0.31	0.32	0.18	0.25	0.26	0.19	0.26	0.27
F(s)[c]	1.90	1.90	1.90	1.93	1.92	1.92	1.93	1.92	1.92
F(p)[c]	5.56	5.57	5.57	5.68	5.68	5.68	5.71	5.71	5.71
s(E)[d]	1.925	1.882	2.010	1.885	1.802	1.924	1.894	1.810	1.936
s(M)[d]	0.008	0.077	−0.071	0.082	0.175	0.039	0.080	0.195	0.044
s(F)[d]	0.023	0.014	0.021	0.011	0.008	0.012	0.009	0.002	0.007
μ[e]	0.15	1.05	1.28	0.39	0.59	0.79	0.54	0.49	0.70
ΔE[f]	274	313	319	122	138	169	150	191	197

[a] Bond lengths and angles are in Å and degrees. All calculations performed at the B3LYP//6-311+G(2d)/SDD level. [b] Mulliken atomic/Natural charges. [c] Natural electron configuration for valence orbitals. [d] Mulliken atomic spin densities: value given for only one fluorine atom. [e] Molecular dipole moment in D. [f] Binding energy in kcal/mol relative to M + EF_3.

Ti−F, and within 2% on either side for Zr−F and Hf−F modes.[18,32] The observed and calculated frequencies in Table 1 fit even better than this relationship, which substantiates our identification of these new triplet state nitrene molecules. The observed and calculated infrared intensities are also qualitatively correct. Notice the reversal in the order of antisymmetric and symmetric M−F stretching frequencies with increasing metal mass between Zr and Hf, and this is also matched by our calculations.

Notice that the M÷N stretching frequencies for the group 4 nitrene series at 596.7, 553.1, and 548.1 cm^{-1} are significantly lower than the M≡N stretching frequencies for the group 6 nitride series at 1015, 1075, and 1091 cm^{-1}, respectively, although the analogous M−F stretching frequencies differ by less than 50 cm^{-1}.[15] Observed frequencies for the N÷ZrF_3 and N÷HfF_3 molecules may be compared with those for the isoelectronic HC÷ZrF_3 [659.7, antisym; 651.7, sym; 627.6 cm^{-1}, C−Zr str] and HC÷HfF_3 [648.6, sym; 642.9, antisym; 621.7 cm^{-1};

Table 5. Description of the E÷M Bonding Molecular Orbitals for Triplet State Terminal Pnictinidenes E÷MF_3 (E = N, P, As, M = Ti, Zr, Hf)[a]

m. o.[b]	N÷TiF_3	P÷TiF_3	As÷TiF_3	N÷ZrF_3	P÷ZrF_3	As÷ZrF_3	N÷HfF_3	P÷HfF_3	As÷HfF_3
σ_α	77%N,23%Ti	62%P,38%Ti	60%As,40%Ti	82%N,18%Zr	68%P,32%Zr	67%As,33%Zr	83%N,17%Hf	69%P,31%Hf	68%As,32%Hf
σ_β	67%N,33%Ti	54%P,46%Ti	51%As,49%Ti	77%N,23%Zr	64%P,36%Zr	62%As,38%Zr	78%N,22%Hf	66%P,34%Hf	64%As,36%Hf
π_α	89%N,11%Ti	86%P,14%Ti	87%As,13%Ti	100%N,0%Zr	88%P,12%Zr	88%As,12%Zr	100%N,0%Hf	89%P,11%Hf	89%As,11%Hf
π_α	89%N,11%Ti	86%P,14%Ti	87%As,13%Ti	100%N,0%Zr	88%P,12%Zr	88%As,12%Zr	100%N,0%Hf	89%P,11%Hf	89%As,11%Hf

[a] All calculations performed at the B3LYP//6-311+G(2d)/SDD level. Natural bond orbital analysis employed. [b] Bonding molecular orbital occupancies greater than 0.98 electron. Electron spins are indicated α and β. The π molecular orbitals are degenerate and are dominated by pnictide p (100%) and metal d (>79%) atomic orbitals.

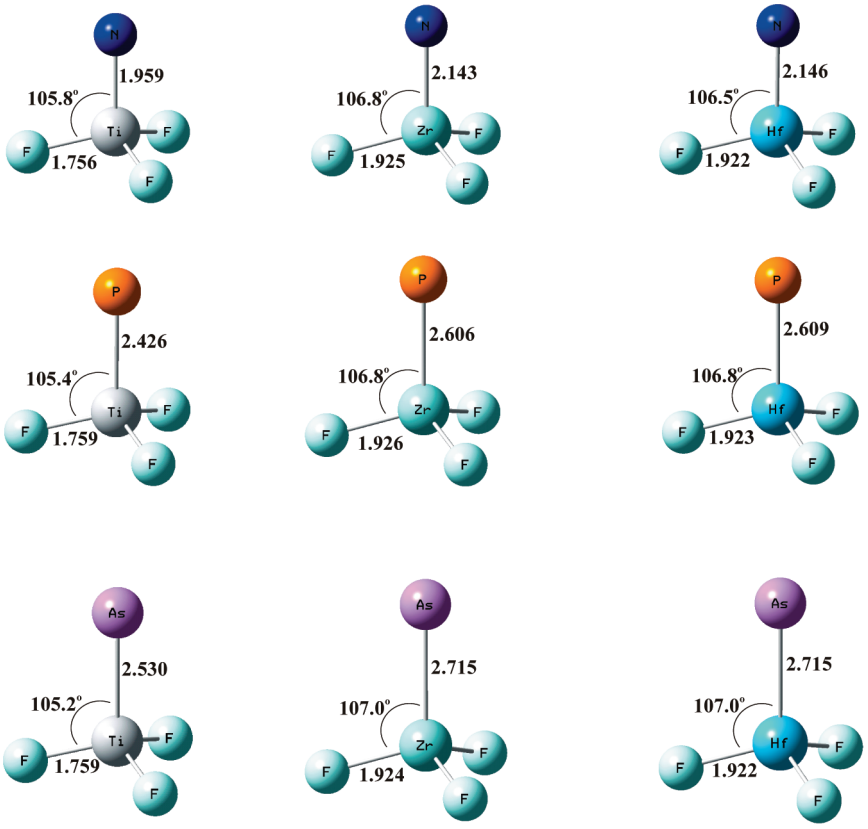

Figure 4. Structures calculated for nine group 4 transition metal trifluoride pnictinidenes using B3LYP/6-311+G(2d)/SDD methods.

C−Hf str] triplet state species.[32] The four observed M−F stretching frequencies for the N÷M nitrenes are 1−18 cm^{-1} higher than for the C÷M species, but the C−Zr stretching frequency is 74.5 cm^{-1} higher than the N−Zr stretching mode and the C−Hf frequency is 73.6 cm^{-1} above the N−Hf value. These consistent frequency trends for closely related isoelectronic molecules substantiate our assignments.

A major contribution to the energy differences between the last steps of reaction 1 is the strong M−F bonds compared to weak N−F bonds. An interesting comparison can be made between the isoelectronic HN=CH_2 and N÷CH_3 reactive species. The latter is computed at the B3LYP level to be 50 kcal/mol higher in energy, and a major factor here is the single N−C bond compared to the N=C bond. However, in contrast, as mentioned above the trifluorotitanium nitrene is more stable (39 kcal/mol) than the FN=TiF_2 imine isomer owing to the stronger Ti−F bond.

Identification of the P÷MF_3 molecules. Phosphorus trifluoride is less reactive, and the infrared spectra contain fewer absorptions. The overall reaction 2 is less exothermic: the final products are 122, 138, and 169 kcal/mol lower in energy that the reagents.

$$M(^3F) + PF_3 \rightarrow F_2P-MF \rightarrow FP{=}MF_2 \rightarrow P \div MF_3 \quad (2)$$

For the Ti reaction, new Ti−F stretching absorptions at 769.0 and 688.2 cm^{-1} fall 13−17 cm^{-1} lower in frequency than the nitrene product, but the strong product bands with Zr are only 3−7 cm^{-1} lower than the nitrene values as the heavier metal mediates the group 15 mass change. Notice the reversal in mode intensities for the Hf product at 662.6 and 647.4 cm^{-1} as the symmetric and antisymmetric M−F_3 stretching mode positions reverse. This relationship is in accord with our vibrational frequency calculations (Table 2).

Identification of the As÷MF_3 molecules. Arsenic trifluoride is intermediate in reactivity, as attested by the intermediate yield of $TiF_{2,3,4}$ and HfF_4, and the overall reaction energetics. Reaction (3) is 150, 191, and 197 kcal/mol exothermic for the three metals, respectively. The spectra in Figure 3 reveal one new metal dependent product band for each metal, at 765.9 cm^{-1} for Ti, at

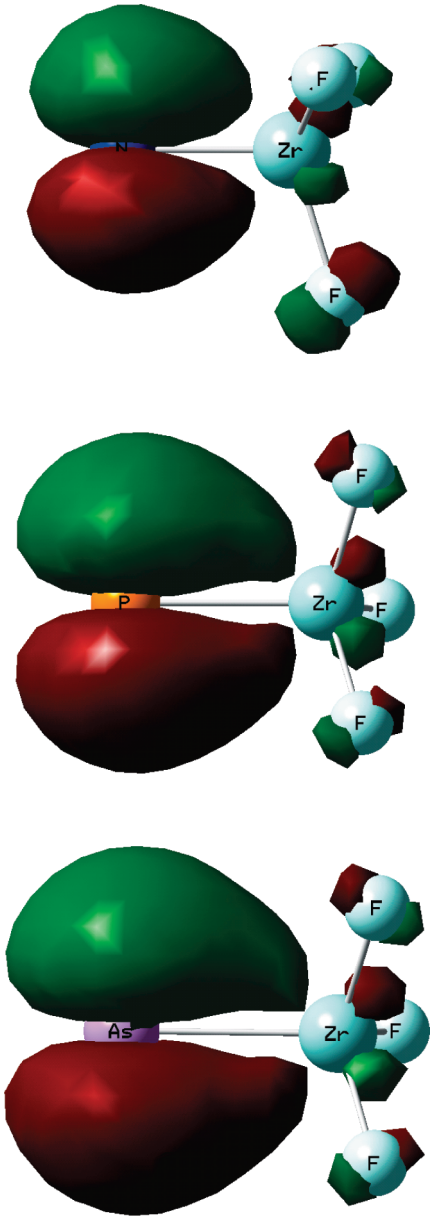

Figure 5. One of the weak degenerate π molecular orbitals calculated for the pnictinidene series N÷ZrF_3, P÷ZrF_3, and As÷ZrF_3 using B3LYP/6-311 + G(2d)/SDD methods and plotted with an iso-electron density of 0.03 e/au^3.

663.6 cm^{-1} for Zr, and at 646.9 cm^{-1} for Hf. These bands fall stepwise in line below the analogous NMF_3 and PMF_3 product antisymmetric M−F stretching frequencies (Tables 1 and 2) as the heavier transition metal dampens the effect of pnictide substitution. Our DFT predictions for the strongest infrared absorption correlate very closely[24,25] with the observed absorptions (Table 3).

Bonding in the Terminal Pnictinidenes. Natural bond orbital analysis[26] was performed for the group 4 metal terminal pnictinidene series, and the results are outlined in Tables 4 and 5. The first point to notice is that the Mulliken atomic electron spin densities on the N, P, and As centers are 1.8 or greater indicating clearly that there is only a small amount of (p-d) π bonding interaction in these triplet ground-state molecules. Perhaps the most interesting finding is that the lowest of these group 15 spin densities, 1.802 and 1.810, are on P in the Zr and Hf phosphinidines, and the metals have spin densities of 0.175 and 0.195, respectively. This combination represents the most favorable (p-d) π orbital overlap. Even so the (p-d) π molecular orbitals are dominated by the P atom with 88 and 89% contributions from P 3p (Table 5). Both the smaller N 2p and the larger As 4p valence orbitals are less effective than the P 3p orbitals. Although (p-d) π bonding is more important for N than P, this is based largely on interaction with first row elements.[33,34] When the partner is an early transition metal *n*d orbital, P 3p dominates the (p-d) π bonding scene.

Another comparison of interest is with the isoelectronic HC÷MF_3 molecules, which have been prepared by the analogous reactions with fluoroform,[32] where the computed HC÷MF_3 and N÷MF_3 bond lengths are almost the same (within 0.02 Å). The analogous calculation for HC÷TiF_3 finds 1.837 and 0.123 spin densities on C and Ti, which may be compared with the 1.925 and 0.008 values given for N÷TiF_3 in Table 4. In addition, natural bond orbital calculations find that the more diffuse C 2p orbital overlaps more effectively than N 2p with Ti 3d, and the π_α molecular orbitals are 79% C and 21% Ti, which shows more interaction than the 89% N and 11% Ti π_α molecular orbitals for N÷TiF_3 (Table 5). Although the spin densities for N (1.885) and Zr (0.082) indicate electron transfer, the computed molecular orbitals are 100% N, but the bonding situation is more favorable for C with Zr as the C (1.894) and Zr (0.115) spin densities and the π_α MO 85% C and 15% Zr indicate. Similarly, the C (1.921) and Hf (0.094) spin densities for HC÷HfF_3 are near the nitrene values (Table 4), but the π_α molecular orbitals are 86% C as compared to 100% N (Table 5, Figures 4, 5).

Conclusions

The NF_3, PF_3, or AsF_3 molecules react with laser-ablated Ti, Zr, and Hf atoms to produce triplet state terminal pnictinidene N÷MF_3, P÷MF_3, or As÷MF_3 molecules, which are trapped in an argon matrix and identified by their infrared spectra and comparison to computed vibrational frequencies. Density functional theory calculations converge to C_{3v} symmetry triplet state structures with relatively long terminal group 15-group 4 bonds for these lowest energy reaction products. The two unpaired electrons in nitrogen 2p, phosphorus 3p, or arsenic 4p orbitals are shared to various degrees with empty metal *n*d orbitals leading to very weak degenerate π molecular orbitals based on DFT bonding orbital analysis and spin density calculations. This weak π bonding interaction with early transition metal group 4 *n*d orbitals appears to work best with Zr and Hf with phosphorus 3p orbitals, and almost as well for arsenic 4p orbitals. Although there are more terminal nitride than phosphide complexes, and even fewer arsenide complexes,[35] our work suggests that phosphinidenes and even arsinidenes can be stabilized by early transition metal complexes in macroscopic reactions.

Acknowledgment. We gratefully acknowledge financial support from NSF Grant CHE 03-52487 and NCSA Grant CHE07-0004N to L.A.

(33) Cotton, F. A.; Wilkinson, G.; Murillo, C. A.; Bochmann, M. *Advanced Inorganic Chemistry*, 6th ed.; Wiley: New York, 1999.
(34) Massey, A. G. *Main Group Chemistry*, 2nd ed.; John Wiley and Sons: New York, 2000.
(35) Balazs, G.; Gregoriades, L. J.; Scheer, M. *Organometallics* 2007, *26*, 3058; and references therein.